**Title**

Silica-gelatin hybrid sol-gel coatings: a proteomic study with biocompatibility implications

**Authors**

N. Araújo-Gomes[1,2]*, F. Romero-Gavilán[1]*&, I. Lara-Sáez[1], F. Elortza[3], M. Azkargorta[3], I. Iloro[3], M. Martínez-Ibañez[4], J.J. Martín de Llano[5], M. Gurruchaga[4], I. Goñi[4], J. Suay[1], A.M. Sánchez-Pérez[2]

[1] Departamento de Ingeniería de Sistemas Industriales y Diseño. Universitat Jaume I, Av. Vicent-Sos Baynat s/n. Castellón 12071. Spain.

[2] Department of Medicine. Universitat Jaume I, Av. Vicent-Sos Baynat s/n. Castellón 12071. Spain.

[3] Proteomics Platform, CIC bioGUNE, CIBERehd, ProteoRed-ISCIII, Bizkaia Science and Technology Park, 48160 Derio, Spain.

[4] Facultad de Ciencias Químicas. Universidad del País Vasco. P. M. de Lardizábal, 3. San Sebastián 20018. Spain.

[5] Department of Pathology and Health Research Institute of the Hospital Clínico (INCLIVA), Faculty of Medicine and Dentistry, University of Valencia, 46010 Valencia, Spain

*Co-authorship.

**Corresponding author:**

Francisco Romero-Gavilán (phone: +34 667303550; e-mail: gavilan@uji.es)

**Abstract**

Osseointegration, including the foreign body reaction to biomaterials, is an immune-modulated, multifactorial, and complex healing process in which various cells and mediators are involved. The buildup of the osseointegration process is immunological and inflammation-driven, often triggered by the adsorption of proteins on the surfaces of the biomaterials and complement activation.

New strategies for improving osseointegration use coatings as vehicles for osteogenic biomolecules delivery from implants. Natural polymers, such as gelatin, can mimic collagen I and enhance the biocompatibility of a material. In this experimental study, two different base sol-gel formulations and their combination with gelatin, were applied as coatings on sandblasted, acid-etched titanium (SAE-Ti) substrates and their biological potential as osteogenic biomaterials was tested. We examined the proteins adsorbed onto each surface and their *in vitro* and *in vivo* effects. *In vitro* results showed an improvement in cell proliferation and mineralization in gelatin-containing samples. *In vivo* testing showed the presence of a looser connective tissue layer in those coatings with substantially more complement activation proteins adsorbed, especially those containing gelatin. Vitronectin and FETUA, proteins associated with mineralization process, were significantly more adsorbed in gelatin coatings.

## 1. Introduction

The regenerative processes in the bone entail responses to continuous biological challenges. The sequence of bone induction and conduction events, involving various types of cells and signaling pathways in a determined order, is necessary to achieve an ideal regeneration (Dimitriou et al. 2011). The implants used in the field of bone regeneration have been continuously studied and optimized since the last century. The results of implantation depend largely on the deposition of signaling proteins onto the surface of a biomaterial and will define the magnitude and type of the reaction (specially inflammatory, immune, and coagulation) of the host to the foreign body implantation (Wilson et al. 2005).

The complement cascade is involved in a variety of physiological and pathophysiological processes, apart from its role as an immune effector. This cascade also regulates the cellular turnover, healing, proliferation, and regeneration (Rutkowski et al. 2010). The disproportionate long-term effects are generally interpreted as implant rejection events. These responses involve mostly uncontrolled blood coagulation processes, the development of infection, and the formation of immune structures (*e.g.* fibrous capsule) surrounding the foreign body and infected or damaged tissue.

Biomaterials are manufactured and tested to improve the life quality of the patient by minimizing the impact of the implanted foreign body and achieving the recovery in the shortest time possible (Duffield et al. 2008; Boehler et al. 2011). Assessing the viability of biomaterials involves a battery of extensive tests before the final product can be released to the market; these tests normally entail both *in vitro* and *in vivo* procedures. *In vivo* testing is the ideal standard in new biomaterial trials as it examines their effects on a living organism. However, *in*

*vitro* testing is the first and necessary step to exclude the immediate damage to the organism; it can also help to avoid the ethical problems and minimize the costs. However, the *in vivo* results often do not reflect the *in vitro* outcomes. This problem is invariably emphasized by the experts in the field of regenerative bone engineering. Thus, new approaches and tools are needed to avoid detrimental side effect and predict the efficacy of biomaterials (Hulsart-Billström et al. 2016).

Silica sol-gel hybrid materials are often used in biomedical applications due to the relative ease of controlling their degradation kinetics and the network pore size. These materials degrade by releasing silicon compounds in the $Si(OH)_4$ form to the surrounding microenvironment, providing a good osteogenic setting for the new bone tissue formation (Juan-Díaz et al. 2014; Romero-Gavilán et al. 2016; Juan-Díaz et al. 2016). Moreover, the process itself results in a good grade of purity at low temperatures. Gelatin is occasionally embedded in the surface of the biomaterial to favor biocompatibility, cell adhesion, proliferation and differentiation (Chen et al. 2009; Shue et al. 2012) because it can mimic the chemical and biological functions of collagen I in a living organism (Chan et al. 2015).

In the silicon networks, gelatin can be effectively crosslinked with an inorganic sol-gel alkoxysilane matrix without losing its osteogenic properties (Yoon et al. 2008). This is useful for controlling the degradation rate, and gelatin can be used as a therapeutic agent in the matrix under mild conditions (Kuijpers et al. 1998; Di Silvio & Bonfield 1999). Different gelatin-silica composites have been developed and studied, and good biocompatibility of these systems has been demonstrated (Smitha, Shajesh, et al. 2007; Lei et al. 2013; Lei et al. 2014; Mahony et al. 2014). Lei et al. have set silica-gelatin hybrid implants using

3-glycidoxypropyl-trimethoxysilane (GPTMS) and tetraethoxysilane (TEOS) alkoxysilanes as precursors. Biological assays have shown that these materials have good biocompatibility and they enhance cell proliferation (Lei et al. 2013; Lei et al. 2014).

In a previous work sol-gel compositions with gelatine physically or chemically entrapped were sinthetized, achieving different physico-chemical properties (Martinez-Ibañez et al. 2018). The protein adsorption onto these gelatin-silica networks was studied with quartz crystal microbalance using monoprotein solutions and distinct affinities were detected when the gelatin was present (Martínez-Ibáñez et al. 2017).

In this experimental study, two sol-gel coating bases and their silicon-gelatin correspondents were applied as coatings on sandblasted, acid-etched titanium disc substrates/implants (SAE-Ti), and their biological potential as biomaterials was tested. The compositions with gelatin and their respective base materials were incubated with human serum, simulating a more real setup. Their effects on the adsorbed protein layer using mass spectrometry (LC-MS/MS) were examined, and the *in vitro* and *in vivo* outcomes were studied.

## 2. Materials and methods

### 2.1. Titanium discs

Ti discs (12 mm in diameter, 1-mm thick) were made from a bar of commercially available, pure, grade-4 Ti (Ilerimplant S.L., Lleida, Spain). To obtain the sandblasted, acid-etched (SAE) Ti, the discs were abraded with 4-µm aluminum oxide particles and acid-etched by submersion in sulfuric acid for 1 h to simulate a moderately rough implant surface. Discs were then washed in acetone, ethanol,

and 18.2-Ω purified water (for 20 min in each liquid) in an ultrasonic bath and dried under vacuum. Finally, all Ti discs were sterilized using UV radiation.

## 2.2. Sol-gel synthesis and sample preparation

The silica-gelatin hybrid coatings were obtained through the sol-gel route. The precursor alkoxysilanes used were methyltrimethoxysilane (MTMOS), 3-(glycidoxypropyl)-trimethoxysilane (GPTMS) and tetraethyl orthosilicate (TEOS) (Sigma-Aldrich, St. Louis, MO, USA). Four different compositions were synthesized. We obtained two silica materials with molar percentages of 70% MTMOS and 30% TEOS (70M30T) and 35% MTMOS, 35% GPTMS, and 30% TEOS (35M35G30T). Their respective composites (70M30T-GEL and 35M35G30T-GEL) were made with 0.9% (weight relative to the amount of alkoxysilane) of gelatin from porcine skin (Sigma-Aldrich, St. Louis, MO, USA). The two gelatin-free compositions were synthesized using 2-Propanol (Sigma-Aldrich, St. Louis, MO, USA) as solvent at a volume ratio (alcohol:siloxane) of 1:1. Hydrolysis of alkoxysilanes was carried out by adding (at a rate of 1 drop s$^{-1}$) the corresponding stoichiometric amount of 0.1M HNO$_3$ acid aqueous solution (Panreac, Barcelona, Spain). The solution was kept for 1 h under stirring and then 1 h at rest. The materials with gelatin were prepared using a mixture of 50% 2-Propanol and 50% distilled water as a solvent at a volume ratio (solvent:siloxane) of 1:1. After adding the alkoxysilane precursors, the hydrolysis was carried out by adding (at 1 drop s$^{-1}$) the stoichiometric amount of 0.1M HCl acidified aqueous solution (Panreac, Barcelona, Spain) with the dissolved gelatin. The solution was kept 1 h under stirring and then 1 h at rest, at 37 °C. The samples were prepared immediately afterward. SAE-titanium was used as a substrate. The coating was performed employing a dip coater (KSV instrument-KSV DC). Discs and implants

were immersed in the corresponding sol-gel solution at a speed of 60 cm min$^{-1}$, left immersed for one minute, and removed at a 100 cm min$^{-1}$. Finally, the samples were cured for 2 h at 80 ºC.

## 2.3.  *Physicochemical characterization of coated titanium discs*

A mechanical profilometer Dektak 6M (Veeco, NY, USA) was used to determine the roughness. Two coated discs of each composition were tested. Three measurements were performed for each disc to obtain the average values of the Ra parameter. The contact angle was measured using an automatic contact angle meter OCA 20 (Dataphysics Instruments, Filderstadt, Germany). Ten μL of ultrapure water W04 were deposited on the sol-gel coated surface at a dosing rate of 27.5 μL s$^{-1}$ at room temperature. Contact angles were determined using SCA 20 software. Five discs of each material were studied, after depositing two drops on each disc. The surface topography of the coatings was characterized using scanning electron microscopy (SEM) employing the Leica-Zeiss LEO equipment under vacuum (Leica, Wetzlar, Germany). Platinum sputtering was applied to make the samples more conductive for the SEM observations.

## 2.4.  *In vitro assays*

MC3T3-E1 (mouse calvaria osteosarcoma cell line) cells were cultured on the sol-gel coated titanium discs at a concentration of $1 \times 10^4$ cells/well, in Dulbecco's modified Eagle's medium (DMEM) with phenol red (Gibco-Life Technologies, Grand Island, NY, USA), 1 % 100× penicillin/streptomycin (Biowest Inc., Riverside, KS, USA), and 10 % fetal bovine serum (FBS) (Gibco-Life Technologies, Grand Island, NY, USA). After incubation for 24 hours at 37 ºC in a humidified (95 %) atmosphere of 5 % $CO_2$, the medium was replaced with an

osteogenic medium composed of DMEM with phenol red 1×, 1 % penicillin/streptomycin, 10 % FBS, 1 % ascorbic acid (5 mg mL$^{-1}$), and 0.21 % β-glycerol phosphate, and incubated again under the same conditions. The culture medium was changed every 48 hours. In each plate, a well with cells at the same concentration (1 × 10$^4$ cells) was used as a control of culture conditions.

The biomaterial cytotoxicity was assessed following the ISO 10993-5 norm, measured by spectrophotometry, by contact of the material extract with the cell line. The 96-Cell Titter Proliferation Assay (Promega®, Madison, WI, USA) was employed to measure the cell viability after 24-h incubation of the cells with the extract. We used one negative control (empty cell well) and a positive control with latex, known to be toxic to the cells. Seventy-percent cell viability was the limit below which a biomaterial was considered cytotoxic.

For measuring cell proliferation, the commercial cell viability assay alamar Blue® (Invitrogen-Thermo Fisher Scientific, Waltham, MA, USA) was used. This kit measures the cell viability on the basis of a redox reaction with resazurin. The cells were cultured in wells with the discs (3 replicates per treatment) and examined following the manufacturer's protocol after 4 days, 8 days, and 14 days. The percentage of reduced resazurin was used to evaluate cell proliferation.

To obtain the samples for total protein measurement (BCA) and ALP activity, the culture medium was removed from the wells, the wells were washed three times with 1 × DPBS, and 100 µL of lysis buffer (0. 2 % Triton X-100, 10 mM Tris-HCl, pH 7.2) were added to each well, obtaining the cell lysate. After being kept on ice for 10 min, the lysate was sonicated and centrifuged for 7 min at 13,300 rpm and the supernatant was used to measure the total protein content and the ALP activity. Each sample was pipetted in triplicate (5 µL per well).

The total protein content was calculated from a standard curve for bovine albumin and expressed as $\mu g\ \mu L^{-1}$, following the manufacturer's instructions, using the colorimetric measurement of BCA at 570 nm on a microplate reader Multiskan FC® (Thermo Scientific®).

The conversion of p-nitrophenylphosphate (p-NPP) to p-nitrophenol was used to assess the alkaline phosphatase (ALP) activity. Sample Aliquots of 0.1 mL were used to carry out the assay. One hundred μL of p-NPP (1 mg $mL^{-1}$) in substrate buffer (50 mM glycine, 1mM $MgCl_2$, pH 10.5) was added to the 100 μL of the supernatant obtained from the lysate. After two hours of incubation in the dark (37 ºC, 5 % $CO_2$), absorbance was measured using a microplate reader at a wavelength of 405 nm. ALP activity was obtained from a standard curve obtained using different solutions of p-nitrophenol and 0.02 mM sodium hydroxide. Results were presented as mmol of p-nitrophenol/hour (mmol PNP $h^{-1}$), and data were expressed as ALP activity normalized by the total protein content ($\mu g\ \mu L^{-1}$) obtained using Pierce BCA assay kit (Thermo Fisher Scientific, Waltham, MA, USA) after 7 and 14 days.

### 2.5. *Statistical analysis*

Data were submitted to one-way analysis of variance (ANOVA) and to a Newman-Keuls multiple comparison post-test, when appropriate. Differences with $p \leq 0.05$ were considered statistically significant.

### 2.6. *In vivo experimentation*

To assess the *in vivo* behaviour to the selected coatings, coated dental implants were surgically placed in the tibia of New Zealand rabbits (*Oryctolagus*

*cunicu*lus). This implantation model is widely used to study the osseointegration of dental implants (Mori et al. 1997). All the experiments were conducted in accordance with the protocols of Ethical Committee of the Valencia Polytechnique University (Spain), the European guidelines and legal conditions laid in R. D. 223/1988 of March 14th, and the Order of October 13rd, 1988 of the Spanish Government on the protection of animals used for experimentation and other scientific purposes. The rabbits were kept under 12-h span darkness-light cycle; room temperature was set at 20.5 ± 0.5 °C, and the relative humidity ranged between 45 and 65 %. The animals were individually caged and fed a standard diet and filtered water *ad libitum*. Dental implants were supplied by Ilerimplant S.L. (Lleida, Spain). They were the internal-connection dental implants, made with titanium grade 4, (trademark GMI), of 3.75-mm diameter and 8-mm length. We used the Frontier model, with SAE surface treatment. Overall, 40 implants were used, 20 uncoated (control) and 5 coated (test samples) with each material. The control and test samples were implanted under the same conditions.

We used 20 rabbits, 5 for each material, with weights between 2000 and 3000 g, of the age near the physical closure (indicative of an adequate bone volume). The implantation period for the experimental model was 2 weeks. Implants were inserted in both left and right proximal tibiae, each animal receiving two implants (one control sample and one test sample). Animals were sedated (chlorpromazine hydrochloride) and prepared for surgery, and then anesthetized (ketamine hydrochloride). A coetaneous incision was made in the implantation site in the proximal tibia. The periosteum was removed, and the osteotomy was performed using a low revolution micromotor and drills of successive diameters

of 2, 2.8, and 3.2 mm, with continuous irrigation. Implants were placed by press-fit, and surgical wound was sutured by tissue planes, washed with saline and covered with plastic spray dressing (Nobecutan, Inibsa Laboratories, Barcelona, Spain). After each implantation period, the animal was euthanized by carbon monoxide inhalation, and the implant screws were retrieved to study the surrounding tissues.

Samples for histological examination were processed following the method described by Peris *et al.* (Peris et al. 1993). Briefly, the samples were embedded in methyl methacrylate, and 25–30 µm thick sections were obtained using EXAKTtechnique (EXAKT Technologies, Inc., Oklahoma, USA). For optical microscopy examination, all the sections were stained using Gomori Trichrome solution.

## 2.7. Adsorbed protein layer

Sol-gel coated titanium discs were incubated in a 24-well plate for 180 min in a humidified atmosphere (37 ºC, 5 % $CO_2$), after the addition of 2 mL of human blood serum from male AB plasma (Sigma-Aldrich, St. Louis, MO, USA).

The serum was removed, and, to eliminate the non-adsorbed proteins, the discs were rinsed five times with $ddH_2O$ and once with 100 mM NaCl, 50 mM Tris-HCl, pH 7.0. The adsorbed protein layer was collected by washing the discs in 0.5 M Triethylammonium bicarbonate buffer (TEAB) with 4 % of sodium dodecyl sulfate (SDS) and 100 mM of Dithiothreitol (DTT). The experimental method was adopted from a study by Kaneko et al. (Kaneko et al. 2011). Four replicates for each biomaterial were obtained. The total protein content of the serum employed to this study was quantified before the experiment (Pierce BCA assay kit; Thermo Fisher Scientific, Waltham, MA, USA), obtaining a value of 51 mg $mL^{-1}$.

## 2.8. Proteomic analysis

Proteomic analysis was performed as described by Romero-Gavilán et al. (Romero-Gavilán et al. 2017), with minor variations. Briefly, the same amount of sample (2/10 of the eluted material) was loaded in each lane for the same experimental conditions. The eluted protein was resolved in polyacrylamide gels; the gels were cut into slices. Each of these slices was digested with trypsin and loaded onto a nanoACQUITY UPLC system connected online to a SYNAPT G2-Si MS System (Waters, Milford, MA, USA). Differential protein analysis was carried out using Progenesis software (Nonlinear Dynamics, Newcastle, UK) as described before (Romero-Gavilán et al. 2017), and the functional annotation of the proteins was performed using PANTHER (www.pantherdb.org/) and DAVID

Go annotation programs (https://david.ncifcrf.gov/). Uniprot (http://www.uniprot.org/) nomenclature was adopted to name the proteins without the ending "_HUMAN".

## 3. Results

### 3.1. Synthesis and physicochemical characterization

Our chosen synthesis parameters allowed us to obtain different materials, all with homogenous surfaces, as can be seen in the SEM micrographs (Fig. 1). The 70M30T coating had different morphology in comparison with 35M35G30T. However, no differences in morphology were detected when gelatin was incorporated in the networks. This agrees with the data obtained using the mechanical profilometer. 70M30T and 70M30T-GEL materials had an average surface roughness (Ra) of 0.77 ± 0.13 and 0.79 ± 0.07 µm, respectively. The compositions 35M35G30T and 35M35G30T-GEL exhibited lower roughness (Ra of 0.51 ± 0.14 µm and 0.58 ± 0.15 µm, respectively). The contact angle measurements (Fig. 2) gave similar values for 70M30T and 35M35G30T coatings. However, the addition of gelatin caused a decrease in wettability on both materials.

### 3.2. In vitro assays

None of the biomaterials tested was cytotoxic. After 7 days of incubation, we found no differences between the ALP activities for the examined materials or even between these materials and SAE-Ti. Interestingly, after 14 days, we observed a significant increase in the ALP activity on the material 35M35G30T-GEL in comparison with the other formulations even though this material had the lowest activity after 7 days (Fig. 3). After 14 days, cell proliferation increased

slightly on the formulations with gelatin in comparison with their base materials; the cultures grown on the formulation 70M30T-GEL showed higher levels of proliferation than the control cells. We noted that the proliferative potential of 70M30T base material was better than the proliferative properties of 35M35G30T.

## 3.3. In vivo assays

Titanium implant coatings generated a distinctive tissue response at the experimental time tested. In the screw grooves corresponding to the cortical region no new bone tissue was observed in 70M30T and 35M35G30T coated implants. When implants were coated with a mixture of gelatin combined with either of the two sol-gel solutions new bone tissue growing was observed filling the grooves. From the cortical bone new bone trabeculae grew towards the implant surface region located in the medullary cavity. The relative length of the trabeculae as well as their density was slightly higher for the 70M30T implants when compared to the other 3 experimental groups (Fig. 4). Furthermore, in the medullary cavity a fibrous connective tissue was developed also around the implant surface of the 70M30T samples, containing arterial vessels. The connective tissue was looser and the arterial vessels density lower around 35M35G30T coated implants and those implants coated with a formulation containing gelatin. The inflammatory response was lower for the 70M30T coating considering the relative density and size of giant multinucleated cells laying the implant coating. Thus, few osteoclast-like and multinucleated giant cells, most of them of a small size were observed in the grooves of the implant (Fig. 5a). The relative density of giant cells was slightly higher for the 35M35G30T-coated implants. The addition of gelatin to the sol-gel coating was related to an evident

increase of the giant cells size and cell density, that was about 3- and 4-times higher for the 70M30T- and 35M35G30T-GEL (Fig. 5b) coatings, respectively.

## 3.4. Proteomic analysis

The proteins eluted from each biomaterial were studied using LC-MS/MS. The Progenesis QI software was employed to compare the characteristic proteins adhering to the different surfaces. One hundred seventy-one proteins were detected and quantified for each surface coating.

The comparison of identified proteins on the 70M30T and 35M35G30T materials displays 6 proteins more absorbed onto the 35M35G30T coating (Table 1). While CLUS, FA12 and APOA5 proteins are more abundant on the 70M30T coating. The comparison of the data obtained for the 70M30T and 70M30T-GEL materials reveals 5 proteins with increased adsorption to the composition with gelatin (C1QA, FINC, FETUA, LDHB, and CO8B), while only one (K2C71) is more abundant on the 70M30T coating (Table 2).

The PANTHER diagram showing classification by function is displayed in Fig. 6. Although the 70M30T material yielded only one differentially adhering protein (keratin), adding gelatin to the matrix induced the adhesion of proteins related with the immune system (14%) and the biological adhesion (14%).

Similarly, Table 3 shows the comparison between the compositions 35M35G30T and 35M35G30T-GEL. In this case, 9 proteins were identified as more abundant on the composition with gelatin; CFAD, CO6, CRP, CO8B, and APOM were among them. However, the levels of adhering IGJ, CATD, HORN, and FCN2 were significantly higher for the 35M35G30T biomaterial. The GO functional classification of the proteins was performed using PANTHER system. Fig. 7a and

7b show the biological functions of the proteins differentially adsorbed onto 35M35G30T and 35M35G30T-GEL, respectively. It is noteworthy that while the 35M35G30T proteins were only involved in 4 functions, after adding gelatin, we found differentially adhering proteins participating in 9 biological processes. Moreover, for the formulations with gelatin, the proportion of functions associated with immune system processes increased from 14 % to 20 %. The comparison between Table 2 and 3, give us the unique common differentially adhering protein common to the two materials with gelatin, a complement protein C08B. The comparison between the gelatin compositions is presented in Table 4. Sixteen proteins were preferentially adsorbed onto the 35M35G30T-GEL coating (e.g. S10A9, CFAD, CRP, SAMP, C1QC, and VTNC), while only 4 were more abundant on the 70M30T-GEL (APOA, CLUS, APOA5, and IGJ).


## 4. Discussion

The implantation of bone biomaterials triggers an immediate host response, provided by the immune system. Multi-directional pathways and mechanisms are activated, ultimately determining the integration or rejection of the biomaterial. These responses involve interactions between three types of components: the host immune cells, the host bone cells, and the materials themselves (Chen et al. 2015). The initial layer of proteins adsorbed onto the biomaterial surface will ultimately define its biocompatibility, triggering, among other processes, coagulation, immune and angiogenesis signaling cascades. Hence, each biomaterial, depending on its chemical and physical composition, conformation, and intrinsic characteristics, can adsorb distinct sets and quantities of proteins to its surface. Titanium has been widely used as the base material for implants

16

because of its bioinertia and osteoconductive characteristics (Buser et al. 1991). Nowadays, various coatings are deposited onto this material to confer bioactive properties that enhance and accelerate the osseointegration in a living organism (Jones 2001). Our experimental work focused on the characterization of the protein layer adsorbed onto four distinct biomaterials coated on the titanium discs (*in vitro* assays) or implants (*in vivo* experiments): 70M30T, 70M30T-GEL, 35M35G30T, and 35M35G30T-GEL, and their correlation with *in vitro* and *in vivo* experimentation results. These silica sol-gel hybrid materials were selected because they confer bioactive properties to the titanium surface (Martínez-Ibáñez et al. 2016; Juan-Díaz et al. 2016).

Gelatin-containing formulations were used to examine potential improvements in the biocompatibility as it might enhance the adhesion of the cells by mimicking the behavior of collagen I. Some studies have combined gelatin with other materials with positive bone regeneration properties, such as calcium phosphates or silicon (Kim et al. 2012; Lei et al. 2013; Lei et al. 2014; Mahony et al. 2014) improving the *in vitro* results (Takahashi et al. 2005).

Gelatin was incorporated in both sol-gel base compositions (70M30T and 35M35G30T). In 70M30T, the gelatin is kept in the silica network due to hydrogen bonds between amino and carboxyl groups from gelatin and silanol groups (Smitha, Mukundan, et al. 2007). However, in 35M35G30T, it is anchored to the structure through covalent bonds formed by the reaction with the epoxy ring of the GPTMS precursor (Mahony et al. 2014).

The main chemical difference between the tested base materials (70M30T and 35M35G30T) is the presence of the GPTMS organic groups in the 35M35G30T. In general, physico-chemical results display a decrease on roughness when

GPTMS is added, whereas the incorporation of gelatin in both base materials shows an increase on hydrophobicity, possibly due to the special distribution of hydrophobic groups at the surface. Regardless of these differences, the *in vitro* results show non-significant or non-existent divergences between both base materials. The only exceptions were the increased cell proliferation on the 70M30T-GEL samples (result that it is described in the bibliography (Lei et al. 2013; Lei et al. 2014), and the significant increase in the ALP activity on 35M35G30T-GEL (Fig. 3). However, it is worth mentioning the *in vitro* strategy adopted (using a single immortalized cell line), is not the ideal to simulate the whole *in vivo* setup of an implantation procedure, in which various biological systems and cues are involved, but it is the generally accepted standard for testing biomaterials nowadays. This *in vitro* setup gives the experimentation some clues about the material influence directly on the osteoblastic cell behavior but does not consider parameters like the immune response and coagulative systems, which is something to take into account as a future perspective (Kohli et al. 2018).

Regarding proteomic analysis, it is interesting to observe the correlation between the base material 35M35G30T and 70M30T (Table 1) *in vivo* outcomes and the adsorbed layer of proteins formed onto each surface.  In particular, 35M35G30T-coating shows the formation of a thin fibrous connective tissue surrounding the material. In the mentioned comparative table 1, it is clear the greater adsorption of mainly two proteins directly related with the complement pathway: involved in the classical pathway (C1QA) and the lectin pathway (FCN-2), respectively (Ma et al. 2009).

Interestingly, between 70M30T and 70M30T-GEL (Table 2), is notable a slightly greater adsorption of C1QA when the base material is supplemented with gelatin, which can explain the existence of a very thin sheet of fibrous connective tissue (Fig. 4c). At the same time, it is clear the greater adsorption of FINC on the material with gelatin, which is a protein widely described to be involved on cellular adhesion and proliferative processes (Ruoslahti 1984; Sottile et al. 1998). Notably, the proteins FETUA, CO8B, and C1QC were more abundant on the 70M30T-GEL than on its base material. C1QC and CO8B are pro-inflammatory proteins. However, it is interesting to note that FETUA has been described as a modulator of macrophage opsonization, displaying anti-inflammatory activity, among its other functions. Moreover, this protein has a role in the fibril mineralization and may promote bone tissue formation (Manolakis et al. 2017).

The comparison and characterization of the layers of proteins formed on 35M35G30T and 35M35G30T-GEL coated surfaces (Table 3) showed more proteins related to the immune system adsorbed onto the 35M35G30T-GEL material (Fig. 7), in particular, the proteins CO6, CFAD, CO8B, and CRP, a complement system activator (Murphy et al. 2008). Hence, in this aspect and at this point it is important to confirm the correlation between the greater adsorption of complement proteins and what is observed in regard to the increased presence of multinucleated giant cells around the gelatin-doped materials (Fig. 5), that means that the incorporation of gelatin molecule supposes an increase in the immune response associated to the biomaterial.

It was also observed the increased levels of adsorption (approximately 2-fold) of pro-inflammatory proteins onto the 35M35G30T-GEL in comparison with 70M30T-GEL, namely S10A9 (Narumi et al. 2015), CFAD (Takahashi et al.

2010), CRP, SAMP, C1S, and C1QC (Ricklin et al. 2010). Worthy of note is the enhanced adsorption of VTNC (1.60-fold increase) on the 35M35G30T-GEL. This protein induces the osteogenesis by promoting the osteoblast differentiation, in the same way as collagen I (Salasznyk et al. 2004). This different protein adsorption could be related to both the differences in base material characteristics and the distinct gelatin linking strategies, which could condition the gelatin conformational organization in the network and then the exposure of its functional groups to the serum proteins.

In the *in vivo* experiments connective tissue developed and remained around regions of the implant surfaces not situated in the proximity of bone tissue. Thus, around the medullary cavity portion of 70M30T-coated implants a more fibrous layer was observed. All materials with differentially adsorbed proteins related to the complement system or with complement system activator proteins (35M35G30T and gelatin formulations) developed a looser connective tissue around the implant. Despite of the connective tissue formation, the histology of these materials showed proper bone tissue developing and direct bone-implant contact in some areas. The incorporation of gelatin indeed had some effect on the induction of a better implant integration, as new bone tissue was observed filling the screw grooves on the cortical zone, which is concordant with the hypothesis established above, as far as it enhances the osteoblast proliferation and differentiation. The increased abundance of complement proteins on some of the materials might be sufficiently high to promote the formation of a loose connective tissue layer (e.g. in comparison with more fibrous capsules) but not too high to prevent partially good osseointegration. A non- chronic immune response is not always undesirable as it favors the tissue growth and

regeneration around the implant (Rutkowski et al. 2010). In fact, the role of cytokines is not uniquely limited to the inflammatory response, as they are described to play a role on osteoblastic activation and/or on osteoclast inhibition, thus enhancing bone formation processes (Kitaura et al. 2016).

One way of measuring the grade of the immune reaction to these materials, might be the establishment of an inhibitory/activator ratio of the identified anti-inflammatory proteins, as VTNC, in comparison with the pro-inflammatory protein CRP. Applying these criteria, the data obtained from the proteomic analysis shows a decrease on these ratios, in particular on the materials incorporating gelatin. For example, the ratio VTNC/CRP on the 70M30T material reaches a value of 76.05, whilst the same material supplemented with gelatin as a value of 56.71. The same finding is observed with the 35M35G30T material, although not having such high values.

This might be related with the differences between the base materials. Having into account these ratios, an appropriate equilibrium between anti- and pro-inflammatory proteins can be desirable to avoid a chronic inflammatory response and fibrotic tissue formation. The results obtained from the analysis of this ratio are consistent with the *in vivo* results, in the sense that is visible an increase on the inflammatory reaction with a greater presence of multinucleated giant cells around the gelatin-supplemented coating on both base materials. This might be explained due to the smaller ratio due to the greater adsorption of CRP on them. This fact comes to reinforce the potential of proteomic analysis when addressing material biocompatibility, as documented in a previous study (Araújo-Gomes et al. 2017).

## 5. Conclusions

In summary, it has been shown that the base material 35M35G30T may induce overall a higher immune response than the other base material 70M30T *in vivo*. Although *in vitro* results are not concordant with this behaviour, proteomic analysis show effectively more adsorption of proteins related to the immune/inflammatory response on the base material 35M35G30T. The *in vivo* behaviour displays that 70M30T base material produces a lower immune response at the period tested that increases when adding gelatine while the 35M35G30T formulation induces a higher response that also increases when gelatin is added. Overall, the addition of gelatin on each material's matrix, provide an even greater immune response, supported by the fact of the adsorption of having more pro-inflammatory proteins adsorbed on the gelatin-silica hybrid sol-gel formulations, in particular the CRP, a great activator of the complement cascade. On the equilibrium between pro and anti-inflammatory adsorbed proteins may reside the key for a prediction of *in vivo* outcome.

# REFERENCES

Araújo-Gomes N, Romero-Gavilán F, Sanchez-Pérez AM, Gurruchaga M, Azargorta M, Elortza F, Martínez-Ibáñez M, Iloro I, Suay J, Goñi I. 2017. Characterization of serum proteins attached to distinct sol – gel hybrid surfaces. J Biomed Mater Res B Appl Biomater.:1–9.

Boehler R, Graham J, Shea L. 2011. Tissue engineering tools for modulation of the immune response. Biotechniques [Internet]. 51:239–240. Available from: http://www.ncbi.nlm.nih.gov/pmc/articles/PMC3526814/

Buser D, Schenk RK, Steinemann S, Fiorellini JP, Fox CH, Stich H. 1991. Influence of surface characteristics on bone integration of titanium implants. A histomorphometric study in miniature pigs. J Biomed Mater Res. 25:889–902.

Chan TR, Stahl PJ, Li Y, Yu SM. 2015. Collagen-gelatin mixtures as wound model, and substrates for VEGF-mimetic peptide binding and endothelial cell activation. Acta Biomater. 15:164–172.

Chen KY, Shyu PC, Dong GC, Chen YS, Kuo WW, Yao CH. 2009. Reconstruction of calvarial defect using a tricalcium phosphate-oligomeric proanthocyanidins cross-linked gelatin composite. Biomaterials. 30:1682–1688.

Chen Z, Klein T, Murray RZ, Crawford R, Chang J, Wu C, Xiao Y. 2015. Osteoimmunomodulation for the development of advanced bone biomaterials. Mater Today [Internet]. 19:304–321. Available from: http://dx.doi.org/10.1016/j.mattod.2015.11.004

Dimitriou R, Jones E, McGonagle D, Giannoudis P V. 2011. Bone regeneration: current concepts and future directions. BMC Med [Internet]. 9:1–10. Available

from: http://www.biomedcentral.com/1741-7015/9/66

Duffield JS, Lupher M, Thannickal V, Wynn T. 2008. Host Responses in Tissue Repair and Fibrosis. October. 141:520–529.

Hulsart-Billström G, Dawson JI, Hofmann S, Müller R, Stoddart MJ, Alini M, Redl H, El Haj A, Brown R, Salih V, et al. 2016. A surprisingly poor correlation between in vitro and in vivo testing of biomaterials for bone regeneration: Results of a multicentre analysis. 31:312–322.

Jones FH. 2001. Teeth and bones: Applications of surface science to dental materials and related biomaterials. Surf Sci Rep.

Juan-Díaz MJ, Martínez-Ibáñez M, Hernández-Escolano M, Cabedo L, Izquierdo R, Suay J, Gurruchaga M, Goñi I. 2014. Study of the degradation of hybrid sol–gel coatings in aqueous medium. Prog Org Coatings [Internet]. [cited 2015 Jan 13]; 77:1799–1806. Available from: http://www.sciencedirect.com/science/article/pii/S0300944014002069

Juan-Díaz MJ, Martínez-Ibáñez M, Lara-Sáez I, da Silva S, Izquierdo R, Gurruchaga M, Goñi I, Suay J. 2016. Development of hybrid sol–gel coatings for the improvement of metallic biomaterials performance. Prog Org Coatings [Internet]. [cited 2016 Mar 21]; 96:42–51. Available from: http://www.scopus.com/inward/record.url?eid=2-s2.0-84956678576&partnerID=tZOtx3y1

Kaneko H, Kamiie J, Kawakami H, Anada T, Honda Y, Shiraishi N, Kamakura S, Terasaki T, Shimauchi H, Suzuki O. 2011. Proteome analysis of rat serum proteins adsorbed onto synthetic octacalcium phosphate crystals. Anal Biochem [Internet]. 418:276–285. Available from:

http://dx.doi.org/10.1016/j.ab.2011.07.022

Kim JB, Okudera T, Furusawa T, Sato M, Yan W, Matsushima Y, Unuma H, Sasano T. 2012. In vivo and in vitro biological ef fi cacy of double-layer coating of titanium with gelatin and calcium phosphate. :589–593.

Kitaura H, Kimura K, Ishida M, Sugisawa H, Kohara H. 2016. Effect of Cytokines on Osteoclast Formation and Bone Resorption during Mechanical Force Loading of the Periodontal Membrane Effect of Cytokines on Osteoclast Formation and Bone Resorption during Mechanical Force Loading of. Sci World J. 2014:1–7.

Kohli N, Ho S, Brown SJ, Sawadkar P, Sharma V, Snow M, García-Gareta E. 2018. Bone remodelling in vitro : Where are we headed? Bone [Internet]. 110:38–46. Available from: http://linkinghub.elsevier.com/retrieve/pii/S8756328218300152

Kuijpers AJ, Engbers GHM, Van Wachem PB, Krijgsveld J, Zaat SAJ, Dankert J, Feijen J. 1998. Controlled delivery of antibacterial proteins from biodegradable matrices. J Control Release. 53:235–247.

Lei B, Shin KH, Koh YH, Kim HE. 2014. Porous gelatin-siloxane hybrid scaffolds with biomimetic structure and properties for bone tissue regeneration. J Biomed Mater Res - Part B Appl Biomater. 102:1528–1536.

Lei B, Wang L, Chen X, Chae S-K. 2013. Biomimetic and molecular level-based silicate bioactive glass-gelatin hybrid implants for loading-bearing bone fixation and repair. J Mater Chem B [Internet]. 1:5153–5162. Available from: http://pubs.rsc.org/en/Content/ArticleHTML/2013/TB/C3TB20941E\nhttp://xlink.rsc.org/?DOI=c3tb20941e

Ma YJ, Doni A, Hummelshøj T, Honoré C, Bastone A, Mantovani A, Thielens NM, Garred P. 2009. Synergy between ficolin-2 and pentraxin 3 boosts innate immune recognition and complement deposition. J Biol Chem. 284:28263–28275.

Mahony O, Yue S, Turdean-Ionescu C, Hanna J V., Smith ME, Lee PD, Jones JR. 2014. Silica-gelatin hybrids for tissue regeneration: Inter-relationships between the process variables. J Sol-Gel Sci Technol. 69:288–298.

Manolakis AC, Christodoulidis G, Kapsoritakis AN, Georgoulias P, Manolakis AC, Kapsoritakis AN, Elisavet K. 2017. α 2-Heremans-schmid glycoprotein ( fetuin A ) downregulation and its utility in inflammatory bowel disease. 23:437–446.

Martinez-Ibañez M, Aldalur I, Romero-Gavilán FJ, Suay J, Goñi I, Gurruchaga M. 2018. Design of nanostructured siloxane-gelatin coatings: Immobilization strategies and dissolution properties. J Non Cryst Solids [Internet]. 481:368–374. Available from: https://doi.org/10.1016/j.jnoncrysol.2017.11.010

Martínez-Ibáñez M, Juan-Díaz MJ, Lara-Saez I, Coso A, Franco J, Gurruchaga M, Suay Antón J, Goñi I. 2016. Biological characterization of a new silicon based coating developed for dental implants. J Mater Sci Mater Med. 27:80.

Martínez-Ibáñez M, Murthy NS, Mao Y, Suay J, Gurruchaga M, Goñi I, Kohn J. 2017. Enhancement of plasma protein adsorption and osteogenesis of hMSCs by functionalized siloxane coatings for titanium implants. J Biomed Mater Res - Part B Appl Biomater.:1–10.

Mori H, Manabe M, Kurachi Y, Nagumo M. 1997. Osseointegration of dental implants in rabbit bone with low mineral density. J Oral Maxillofac Surg

[Internet]. [cited 2016 Jun 23]; 55:351–361. Available from: http://linkinghub.elsevier.com/retrieve/pii/S0278239197901245

Murphy K, Travers P, Walport M. 2008. The complement system and innate immunity. Janeway's Immunobiol. 7:61–81.

Narumi K, Miyakawa R, Ueda R, Hashimoto H, Yamamoto Y, Yoshida T, Aoki K. 2015. Proinflammatory Proteins S100A8/S100A9 Activate NK Cells via Interaction with RAGE. J Immunol [Internet]. 194:5539–48. Available from: http://www.ncbi.nlm.nih.gov/pubmed/25911757

Peris JL, Prat J, Comin M, Dejoz R, Vera IRP. 1993. Técnica histológica para la inclusión en metil- metacrilato de muestras óseas no descalcificadas. Rev Española Cirugía Osteoartic. 28:231–238.

Ricklin D, Hajishengallis G, Yang K, Lambris JD. 2010. Complement: a key system for immune surveillance and homeostasis. Nat Immunol [Internet]. 11:785–97. Available from: http://dx.doi.org/10.1038/ni.1923

Romero-Gavilán F, Barros-Silva S, García-Cañadas J, Palla B, Izquierdo R, Gurruchaga M, Goñi I, Suay J. 2016. Control of the degradation of silica sol-gel hybrid coatings for metal implants prepared by the triple combination of alkoxysilanes. J Non Cryst Solids [Internet]. 453:66–73. Available from: http://linkinghub.elsevier.com/retrieve/pii/S0022309316304112

Romero-Gavilán F, Gomes NC, Ródenas J, Sánchez A, , Mikel Azkargorta, Ibon Iloro F, Elortza IGA, Gurruchaga M, Goñi I, Suay  and J. 2017. Proteome analysis of human serum proteins adsorbed onto different titanium surfaces used in dental implants. Biofouling. 33:98–111.

Ruoslahti E. 1984. Fibronectin in cell adhesion and invasion. Cancer Metastasis Rev. 3:43–51.

Rutkowski MJ, Sughrue ME, Kane AJ, Ahn BJ, Fang S, Parsa AT. 2010. The complement cascade as a mediator of tissue growth and regeneration. Inflamm Res. 59:897–905.

Salasznyk RM, Williams WA, Boskey A, Batorsky A, Plopper GE. 2004. Adhesion to Vitronectin and Collagen I Promotes Osteogenic Differentiation of Human Mesenchymal Stem Cells. J Biomed Biotechnol [Internet]. [cited 2016 Feb 23]; 2004:24–34. Available from: http://www.scopus.com/inward/record.url?eid=2-s2.0-3042722241&partnerID=tZOtx3y1

Shue L, Yufeng Z, Mony U. 2012. Biomaterials for periodontal regeneration: a review of ceramics and polymers. Biomatter. 2:271–277.

Di Silvio L, Bonfield W. 1999. Biodegradable drug delivery system for the treatment of bone infection and repair. J Mater Sci Mater Med. 10:653–658.

Smitha S, Mukundan P, Krishna Pillai P, Warrier KGK. 2007. Silica-gelatin bio-hybrid and transparent nano-coatings through sol-gel technique. Mater Chem Phys. 103:318–322.

Smitha S, Shajesh P, Mukundan P, Nair TDR, Warrier KGK. 2007. Synthesis of biocompatible hydrophobic silica-gelatin nano-hybrid by sol-gel process. Colloids Surfaces B Biointerfaces. 55:38–43.

Sottile J, Hocking DC, Swiatek PJ. 1998. Fibronectin matrix assembly enhances adhesion-dependent cell growth. J Cell Sci. 111 ( Pt 1:2933–2943.

Takahashi M, Ishida Y, Iwaki D, Kanno K, Suzuki T, Endo Y, Homma Y, Fujita T. 2010. Essential role of mannose-binding lectin-associated serine protease-1 in activation of the complement factor D. J Exp Med. 207:29–37.

Takahashi Y, Yamamoto M, Tabata Y. 2005. Enhanced osteoinduction by controlled release of bone morphogenetic protein-2 from biodegradable sponge composed of gelatin and β-tricalcium phosphate. Biomaterials. 26:4856–4865.

Wilson CJ, Clegg RE, Leavesley DI, Pearcy MJ. 2005. Mediation of Biomaterial–Cell Interactions by Adsorbed Proteins: A Review. Tissue Eng [Internet]. 11:1–18. Available from: http://www.liebertonline.com/doi/abs/10.1089/ten.2005.11.1

Yoon BH, Kim HE, Kim HW. 2008. Bioactive microspheres produced from gelatin-siloxane hybrids for bone regeneration. J Mater Sci Mater Med. 19:2287–2292.

**TABLES**

**Table 1**. The comparison of proteins differentially adhered to 70M30T and 35M35G30T sol-gel coatings (Progenesis analysis). ANOVA (p-value < 0.05).

| Description | Accession | 70M30T | 35M35G30T | 35M35G30T/ 70M30T |
|---|---|---|---|---|
| Myosin-1 | MYH1_HUMAN | 5,71E+02 | 9,81E+03 | 17,19 |
| L-lactate dehydrogenase B chain | LDHB_HUMAN | 1,00E+04 | 1,22E+05 | 12,18 |
| Glutamate dehydrogenase 1, mitochondrial | DHE3_HUMAN | 8,24E+02 | 7,13E+03 | 8,65 |
| Ficolin-2 | FCN2_HUMAN | 7,05E+03 | 5,84E+04 | 8,28 |
| Complement C1q subcomponent subunit A | C1QA_HUMAN | 3,17E+04 | 9,68E+04 | 3,06 |
| Hemoglobin subunit alpha | HBA_HUMAN | 3,75E+04 | 6,50E+04 | 1,73 |
| Clusterin | CLUS_HUMAN | 6,81E+05 | 4,15E+05 | 0,61 |

| | | | | |
|---|---|---|---|---|
| Coagulation factor XII | FA12_HUMAN | 1,34E+05 | 7,80E+04 | 0,58 |
| Apolipoprotein A-V | APOA5_HUMAN | 5,41E+03 | 2,85E+03 | 0,53 |

**Table 2**. The comparison of proteins differentially adhered to 70M30T and 70M30T-GEL hybrid coatings (Progenesis analysis). ANOVA (p-value < 0.05).

| Description | Accession | 70M30T | 70M30T-GEL | 70M30T-GEL/70M30T |
|---|---|---|---|---|
| Complement C1q subcomponent subunit A | C1QA_HUMAN | 3.17E+04 | 6.71E+04 | 2.12 |
| Fibronectin | FINC_HUMAN | 8.26E+03 | 1.54E+04 | 1.86 |
| Alpha-2-HS-glycoprotein | FETUA_HUMAN | 2.25E+05 | 3.91E+05 | 1.74 |
| L-lactate dehydrogenase B chain | LDHB_HUMAN | 1.00E+04 | 1.74E+04 | 1.73 |
| Complement component C8 beta chain | CO8B_HUMAN | 1.04E+04 | 1.50E+04 | 1.45 |
| Keratin, type II cytoskeletal 71 | K2C71_HUMAN | 8.38E+03 | 5.90E+03 | 0.70 |

**Table 3.** The comparison of proteins adhered to 35M35G30T and 35M35G30T-GEL hybrid coatings (Progenesis analysis). ANOVA (p-value < 0.05).

| Description | Accession | 35M35G30T | 35M35G30T-GEL | 35M35G30T-GEL/35M35G30T |
|---|---|---|---|---|
| Ig kappa chain V-I region Roy | KV116_HUMAN | 2.73E+04 | 7.34E+04 | 2.69 |
| Complement factor D | CFAD_HUMAN | 2.14E+04 | 4.98E+04 | 2.33 |
| Complement component C6 | CO6_HUMAN | 2.15E+04 | 4.91E+04 | 2.28 |
| C-reactive protein | CRP_HUMAN | 6.62E+03 | 1.35E+04 | 2.04 |
| Complement component C8 beta chain | CO8B_HUMAN | 1.05E+04 | 2.13E+04 | 2.02 |
| Ig gamma-3 chain C region | IGHG3_HUMAN | 8.18E+04 | 1.47E+05 | 1.80 |
| Ig kappa chain V-II region Cum | KV201_HUMAN | 5.71E+05 | 9.69E+05 | 1.70 |
| Apolipoprotein M | APOM_HUMAN | 2.84E+04 | 4.74E+04 | 1.67 |

| | | | | |
|---|---|---|---|---|
| Ig kappa chain V-IV region Len | KV402_HUMAN | 3.46E+05 | 5.28E+05 | 1.53 |
| Immunoglobulin J chain | IGJ_HUMAN | 9.79E+04 | 6.99E+04 | 0.71 |
| Cathepsin D | CATD_HUMAN | 3.65E+04 | 1.66E+04 | 0.46 |
| Hornerin | HORN_HUMAN | 8.79E+03 | 2.25E+03 | 0.26 |
| Ficolin-2 | FCN2_HUMAN | 5.84E+04 | 8.79E+03 | 0.15 |

**Table 4.** The comparison of proteins differentially adhered to 35M35G30T-GEL and 70M30T-GEL (Progenesis analysis). ANOVA (p-value < 0.05).

| Description | Accession | 70M30T-GEL | 35M35G30T-GEL | 35M35G30T-GEL/70M30T-GEL |
|---|---|---|---|---|
| Glutamate dehydrogenase 1, mitochondrial | DHE3_HUMAN | 1.35E+03 | 1.67E+04 | 12.39 |
| L-lactate dehydrogenase B chain | LDHB_HUMAN | 1.74E+04 | 1.57E+05 | 9.01 |
| Myosin-1 | MYH1_HUMAN | 2.18E+03 | 6.79E+03 | 3.11 |
| Protein S100-A9 | S10A9_HUMAN | 3.74E+04 | 9.33E+04 | 2.49 |
| Complement factor D | CFAD_HUMAN | 2.13E+04 | 4.98E+04 | 2.34 |
| C-reactive protein | CRP_HUMAN | 6.08E+03 | 1.35E+04 | 2.22 |
| Serum amyloid P-component | SAMP_HUMAN | 2.54E+05 | 5.29E+05 | 2.09 |
| Ig kappa chain V-I region Roy | KV116_HUMAN | 3.79E+04 | 7.34E+04 | 1.93 |
| Ig kappa chain V-III region SIE | KV302_HUMAN | 2.44E+06 | 4.71E+06 | 1.93 |
| Complement C1q subcomponent subunit C | C1QC_HUMAN | 1.09E+06 | 1.90E+06 | 1.75 |
| Ig kappa chain V-II region Cum | KV201_HUMAN | 5.93E+05 | 9.69E+05 | 1.63 |
| Vitronectin | VTNC_HUMAN | 3.45E+05 | 5.50E+05 | 1.60 |
| Gelsolin | GELS_HUMAN | 1.58E+06 | 2.39E+06 | 1.51 |
| Complement C1s subcomponent | C1S_HUMAN | 2.43E+05 | 3.51E+05 | 1.45 |
| Ig gamma-3 chain C region | IGHG3_HUMAN | 1.03E+05 | 1.47E+05 | 1.43 |
| Actin, cytoplasmic 1 | ACTB_HUMAN | 4.88E+04 | 6.78E+04 | 1.39 |
| Immunoglobulin J chain | IGJ_HUMAN | 9.78E+04 | 6.99E+04 | 0.71 |
| Apolipoprotein(a) | APOA_HUMAN | 3.07E+04 | 1.78E+04 | 0.58 |
| Clusterin | CLUS_HUMAN | 9.81E+05 | 5.11E+05 | 0.52 |
| Apolipoprotein A-V | APOA5_HUMAN | 7.21E+03 | 3.71E+03 | 0.51 |

**FIGURE CAPTIONS**
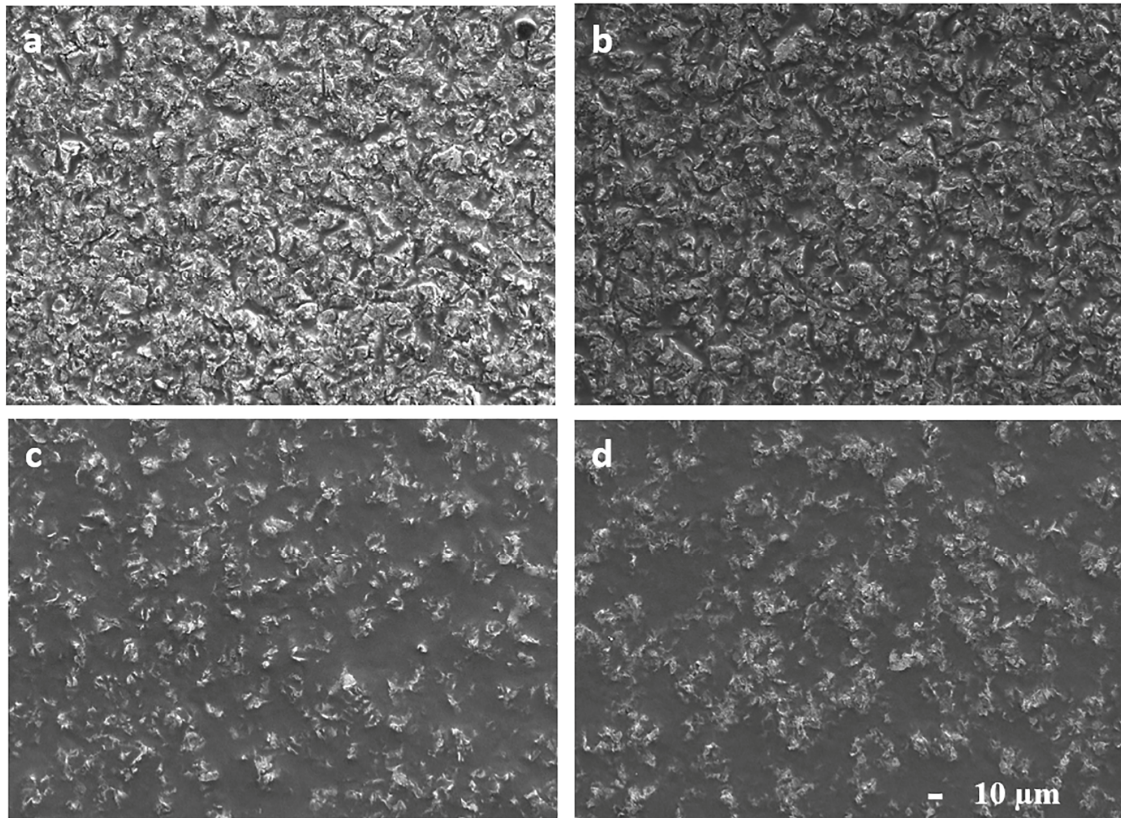


**Figure 1.** SEM images of hybrid sol-gel coatings onto titanium discs: 70M30T (a), 70M30T-GEL (b), 35M35G30T (c) and 35M35G30T -GEL (d). Calibration bar 10 μm.
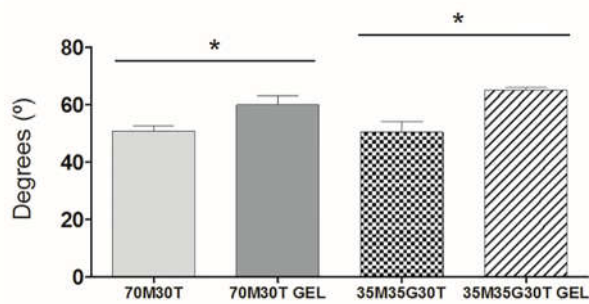


**Figure 2.** Contact angle measurements of 70M30T, 70M30T-GEL, 35M35G30T and 35M35G30T -GEL sol-gel coatings.
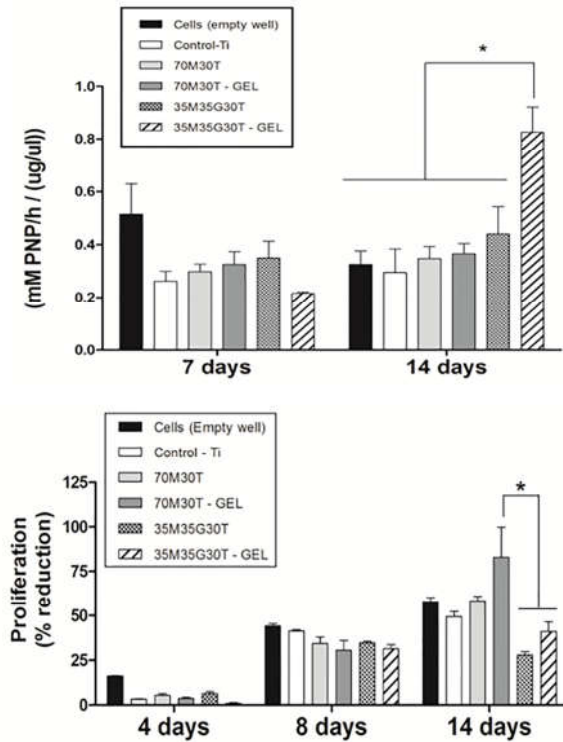
**Figure 3.** MC3T3-E1 in vitro results. (a) ALP activity (mM PNP/h) normalized to the amount of total protein (µg µL-1) levels and (b) proliferation results of the cells cultivated on titanium discs treated with 70M30T, 70M30T-GEL, 35M35G30T, 35M35G30T-GEL formulations. Cells on an empty well without disc were used as a positive control (black column), whereas uncoated titanium discs (white column) were used as a negative control (ANOVA, p ≤ 0,05).
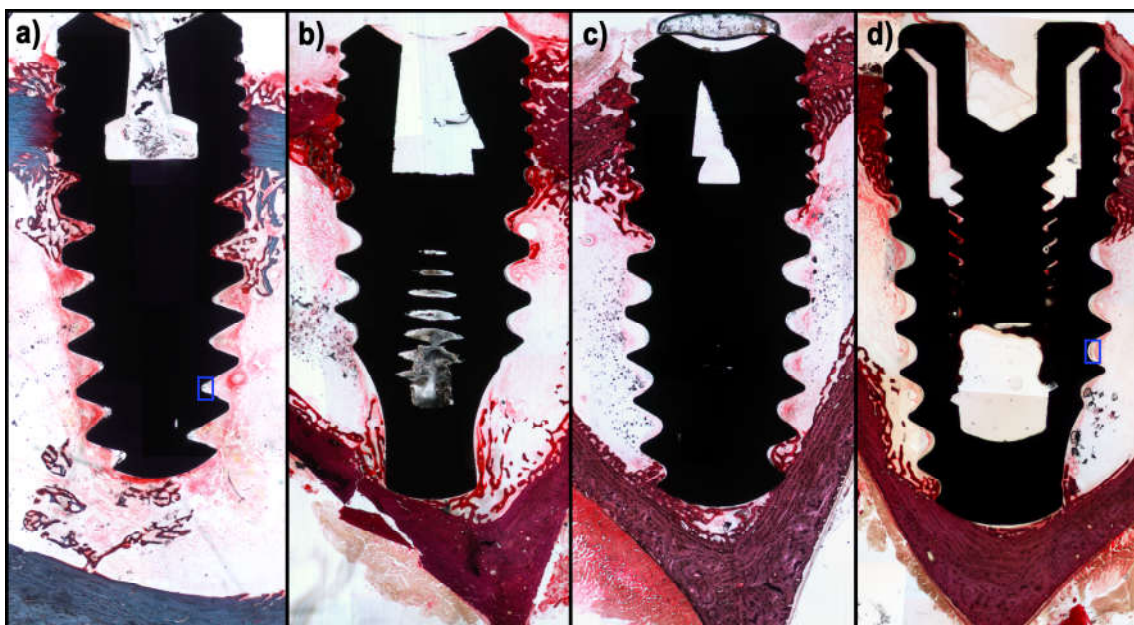
**Figure 4.** Microphotographs of titanium implants. Panoramic images of (a) 70M30T, (b) 70M30T-GEL, (c) 35M35G30T and (d) 35M35G30T-GEL implants. The delineated regions (blue rectangles) in the medullary cavity of (a) and (d) images are shown magnified in Figure 5.
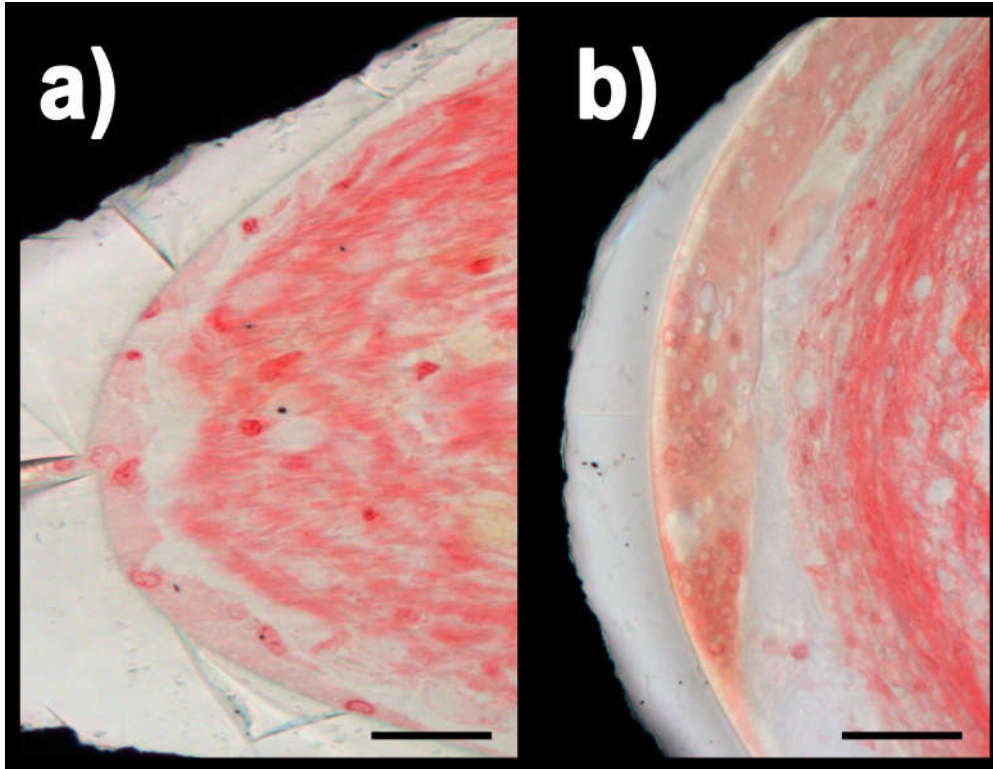


**Figure 5.** Microscopic detail of areas corresponding to the medullary cavity. Multinucleated cells layering the groove surface of (a) 70M30T and (b) 35M35G30T-GEL implants. The areas shown correspond to those delineated in Figure 4. Scale bar, 0.05 mm.
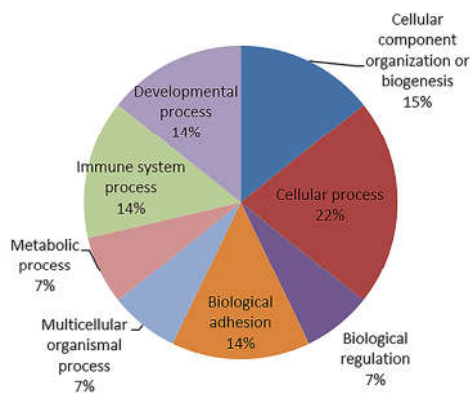
**Figure 6.** PANTHER diagram with the biological process of the proteins differentially adhered to 70M30T-GEL, respect 70M30T.
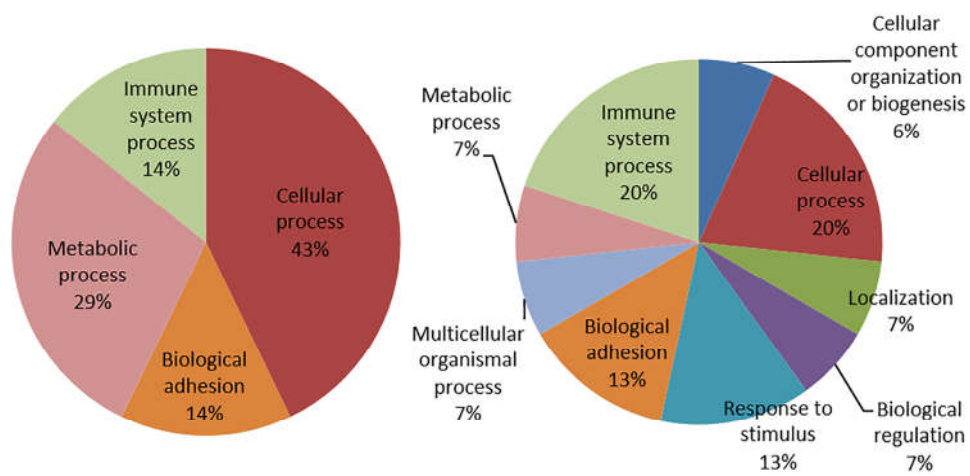


**Figure 7.** PANTHER diagram with the biological process of the proteins differentially adhered to 35M35G30T (a) and 35M35G30T-GEL (b).